Journal of Alloys and Compounds 689 (2016) 481–488

Contents lists available at ScienceDirect

Journal of Alloys and Compounds

journal homepage: http://www.elsevier.com/locate/jalcom

Martensite transformation and magnetic properties of Fe-doped Ni-Mn-Sn alloys with dual phases

Hehe Zhang, Mingfang Qian, Xuexi Zhang*, Longsha Wei, Fuyang Cao, Dawei Xing, Xiping Cui, Jianfei Sun, Lin Geng

School of Materials Science and Engineering, Harbin Institute of Technology, Harbin 150001, China

ARTICLE INFO

Article history:
Received 27 May 2016
Received in revised form
25 July 2016
Accepted 26 July 2016
Available online 29 July 2016

Keywords:
Martensite transformation
Magnetic property
Magnetocaloric effect
Ni-Fe-Mn-Sn alloy

ABSTRACT

Ni-Mn-Sn alloys exhibit high magnetocaloric effect (MCE) during the magnetic-field-induced martensite to austenite phase transformation. However, the low magnetization of the austenite, narrow working temperature interval and high magnetic hysteresis reduced their magnetic refrigeration capacity. Here, the effects of Fe doping on the structural and magnetic transitions of $Ni_{50-x}Fe_xMn_{38}Sn_{12}$ alloys were investigated. The doping of Fe higher than 2.9% induced the occurrence of a secondary γ phase, creating a dual phase alloy. The martensite transformation temperature significantly decreased with the occurrence of the secondary phase. However, the Curie temperatures of both austenite and martensite changed slightly with the formation of the secondary phase. As a result, the magnetostructural coupling, i.e. overlap of the structural and magnetic transitions between the ferromagnetic austenite and the paramagnetic martensite, occurred in the alloys with x = 0.5 - ~4.2. Furthermore, the magnetization of the austenite and martensite both increased with increasing Fe content from x = 0 to x = 5.5, with the magnetization difference between the austenite and martensite saturating at x = 4.2. The dual phase $Ni_{45.8}Fe_{4.2}Mn_{38}Sn_{12}$ alloy, exhibiting a magnetic field dependence of martensite transformation temperature $\Delta T_M/\mu\Delta H$ - 0.28 K/kOe, showed a wider working temperature interval than that of the un-doped $Ni_{50}Mn_{38}Sn_{12}$ alloy. This demonstrated that the $Ni_{45.8}Fe_{4.2}Mn_{38}Sn_{12}$ alloy might exhibit a high magnetic entropy change, wide working temperature interval and low magnetic hysteresis, and thus may be a promising magnetic refrigeration material.

1. Introduction

Ni-Mn-Z (Z = Sn, In and Sb) Heusler alloys [1,2] may be subjected to a metamagnetic transition from the weak magnetic martensite to strong ferromagnetic austenite under an external magnetic field. This makes Ni-Nn-Z (Z = In, Sn and Sb) attractive ferromagnetic shape memory alloys [3] that exhibit the magnetic superelasticity [4], magnetocaloric effect [5,6], magnetoresistance [7,8] and magnetothermal conductivity [9]. The driving force for such metamagnetic transition is attributed to the Zeeman energy $E_{zeeman} = \mu_0 \Delta MH$, where ΔM is the saturation magnetization difference between austenite and martensite phases and H is the strength of the magnetic field. As a result, the E_{zeeman} may be increased by enhancing the ΔM.

However, for $Ni_{50}Mn_{50-x}Z_x$ (Z = Sn, In and Sb) ternary alloys, the effect of heat treatment [10,11] and composition adjustment [12–14] on ΔM is low. For example, the typical ΔM is only ~40 emu/g by tuning the chemical composition of $Mn_{50}Ni_{50-x}In_x$ alloys [15,16]. The Mn-rich $Ni_{50-y}Mn_{(50-x)+y}Sn_x$ alloys exhibit a slightly enlarged ΔM (such as ~55 emu/g at x = 11, y = 7), but an obviously increase in magnetic hysteresis loss (HL) of 168 J/kg [17]. By contrast, the ΔM can be significantly enhanced by a fourth element doping [18–21]. In $Ni_{45}Co_5Mn_{37}In_{13}$ alloy [19], ΔM reached ~90 emu/g, much higher than ~40 emu/g in $Mn_{50}Ni_{50-x}In_x$ alloys, due to the significantly improved austenite magnetization but little change in martensite magnetization [19]. A fourth element doping is also effective in improving MCE by creating magnetostructural coupling state, i.e. the overlap between magnetic and martensite transitions [22]. This was realized by tuning the valence electron concentration *e/a* or changing the unit cell volume [23], which mainly changed the martensite transformation (MT) temperatures. For instance, doping interstitial atoms, such as C, B or H, in Ni-Mn-Z alloys reduced the MT temperatures by increasing the cell volume [21]. On the other hand, substitution by replacement elements,

---

* Corresponding author.
E-mail address: xxzhang@hit.edu.cn (X. Zhang).

http://dx.doi.org/10.1016/j.jallcom.2016.07.282

such as Fe, Co, Cu in Ni-Mn-Z alloys, may increase or decrease MT temperatures, depending on the effect of the fourth element on *e/a* [24].

The intrinsic brittleness is another factor that hinders the engineering application of Ni-Mn-Z alloys. The effect of second ductile phases, distributed mainly at the grain boundary and thus reduced the intergranular fracture tendency, has been demonstrated in Ni-Mn-Z alloys [21,25]. Here, Fe substitution for Ni in $Ni_{50-x}Fe_xMn_{38}Sn_{12}$ ($x = 1.1$, 2.3, 2.9, 4.2, 5.5 and 8.5) alloys were designed and prepared by induction melting, casting and subsequent annealing heat treatments. The critical content of Fe on the occurrence of γ phase, martensite transformation behavior and magnetic transition diagram were investigated. The study showed that $Ni_{50-x}Fe_xMn_{38}Sn_{12}$ alloy exhibited a high magnetization difference between austenite and martensite phases at Fe content $x = 4.2$, as well as low magnetic hysteresis during magnetic-field-induced martensite to austenite transformation, making it an attractive magnetocaloric material.

2. Experimental method

$Ni_{50-x}Fe_xMn_{38}Sn_{12}$ ($x = 1.1$, 2.3, 2.9, 4.2, 5.5 and 8.5, atomic percent) ingots were prepared by induction melting elemental Ni (99.99%), Fe (99.99%), Mn (99.9%) and Sn (99.99%) in an argon atmosphere and casting in a copper mold. The ingots were subsequently sealed in a quartz tube accompanied with Mn powder (to create a Mn vapor atmosphere in the tube) and Ti sheet (acted as oxygen getter), evacuated and back-filled with pure Ar of 25000 Pa and annealed at 1173 K for 24 h. Then the ingots were quenched in iced water. The microstructure and composition were determined by a Zeiss-SUPRA SEM equipped with an Oxford EDS, using 20 kV voltage, 97 μA emission current, 10 mm working distance, 50 μA probe current and >60 s data acquisition time duration using the polished samples. The compositions of the secondary γ phase were determined using large precipitates with size >5 μm. The standard deviation of the composition was obtained based on the results of ~8 spots measurements. The crystal structure of the phases was determined by a Philips X'Pert X-ray diffractometer (XRD) using Cu Kα radiation and a Tecnai G^2 F30 transmission electron microscope (TEM). The magnetization-temperature (*M-T*) and isothermal magnetization (*M-H*) measurements were performed using a vibrating sample magnetometry (VSM) in a commercial magnetic property measurement system (MPMS) of Quantum Design. The *M-T* plots were obtained under heating and cooling rates of 5 K/min. The sample was first cooled down to a low temperature (80 K or 150 K) in a zero field prior to the measurement. A 50 Oe field was then applied and the sample was heated up to 350 K (ZFC). Then, it was cooled back to 80 K or 150 K under 50 Oe (FC). Finally, it was heating up to 350 K under 50 Oe (FH). Magnetic force microscopy (MFM) observations were carried out with a dimension icon scanning probe microscope. The topographic (height contrast) and magnetic (frequency contrast) images were obtained in tapping and tapping-lift mode using standard nonmagnetic and magnetic tips.

3. Results and discussion

3.1. Morphology and crystalline structure of γ phase

Fig. 1 shows the back scattered electron (BSE) micrographs of the annealed $Ni_{50-x}Fe_xMn_{38}Sn_{12}$ ($x = 1.1$, 2.3, 2.9, 4.2, 5.5 and 8.5) alloys. The alloy exhibited a single phase state at Fe content $x = 1.1$ and $x = 2.3$, as shown in Fig. 1a and b. At $x = 2.9$, trace amount of γ precipitates (in dark contrast) appeared in the matrix (in light contrast), as shown in Fig. 1c. However, the content of γ phase dramatically increased at Fe content $x = 4.2$ (Fig. 1d). For even higher content of Fe, i.e. $x = 5.5$ (Fig. 1e) and $x = 8.5$ (Fig. 1f), higher densities of γ phase were formed at the grain boundaries and in the grains. The composition of the matrix alloy and γ phase in $Ni_{50-x}Fe_xMn_{38}Sn_{12}$ ($x = 1.1$, 2.3, 2.9, 4.2, 5.5 and 8.5) alloys are listed in

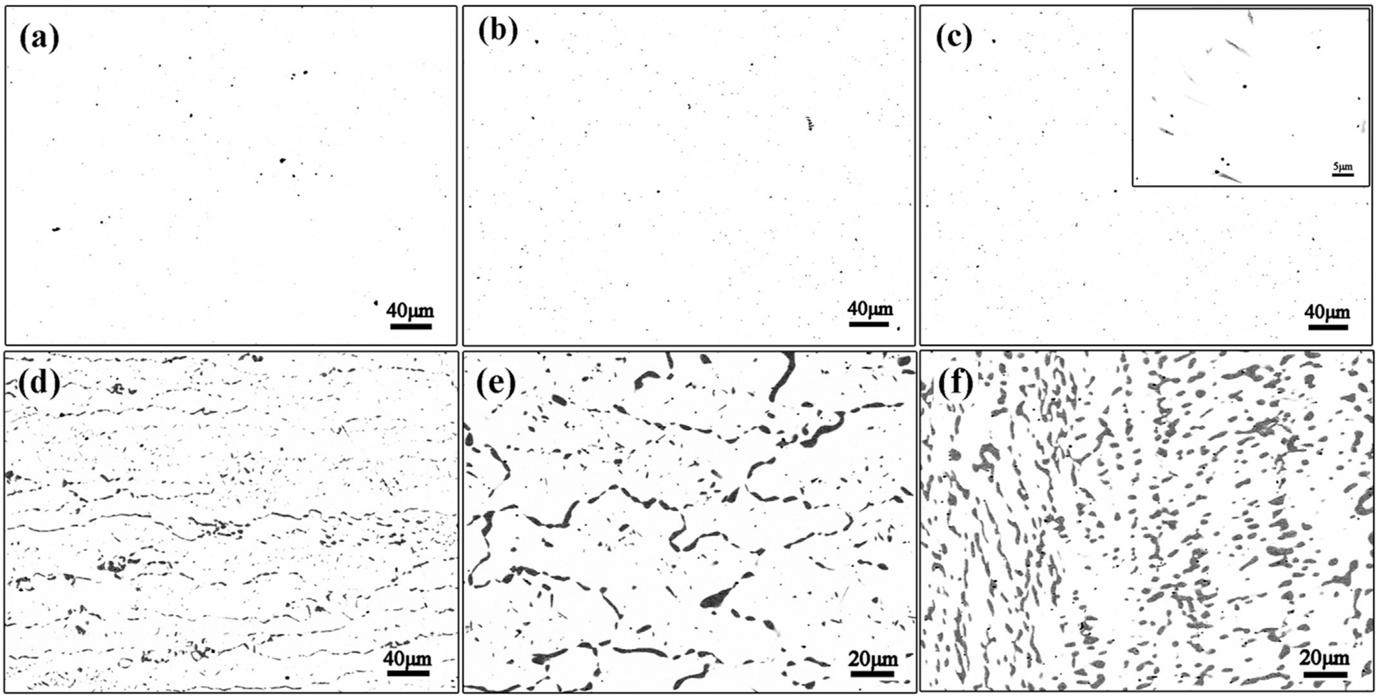

Fig. 1. Back scattered electron (BSE) micrographs showing morphologies of the γ precipitate phase (dark gray) in $Ni_{50-x}Fe_xMn_{38}Sn_{12}$ alloys with Fe doping content of (a) $x = 1.1$, (b) $x = 2.3$, (c) $x = 2.9$, (d) $x = 4.2$, (e) $x = 5.5$ and (f) $x = 8.5$. The inset in (c) shows an enlarged micrograph of the γ phase in the alloy with $x = 2.9$.